Research Article

THE STUDY OF HYDRODYNAMICS ESTIMATION FOR AUTONOMOUS UNDERWATER GLIDERS

P. Jantapremjit[1, *]
P. Prasertsang[1]
P. A. Wilson[2]

[1]*Department of Mechanical Engineering, Faculty of Engineering, Burapha University Mueng, Chonburi, 20131, Thailand*
[2]*Faculty of Engineering and Physical Sciences, University of Southampton, Southampton, SO16 7QF, UK*

ABSTRACT:
Ocean exploration is a challenge which provides knowledge of the environment and ecosystem. Autonomous underwater gliders are advantageous over conventional underwater vehicles. Performance can be evaluated by hydrodynamic characteristics. This paper presents a study of an hydrodynamics estimation for various underwater glider configurations. The designs of hull shape configuration of underwater gliders which is similar to torpedo shape are investigated. The hydrodynamics (drags) are estimated by using computational fluid dynamics. Reynolds-averaged Navier-Stokes equations with the SST model are used to solve this problem. The numerical studies are determined using the open-source software. The work shows results of hydrodynamics comparing a designed underwater glider with the Slocum glider. Performance of the gliders is also evaluated.

Keywords: *Underwater glider, Hydrodynamics, Hull shape*

1. INTRODUCTION

Underwater gliders are capable of travelling through the ocean by utilising the change of buoyancy force and internal moving actuators [1]. Underwater gliders can change their buoyancy from negative to positive in a cyclic manner. Moving mass actuator allows the change of the position of centre gravity and consequently, the pitch angle can be adjusted. They also have external fixed wings and tails which produce stabilsing movement. Lateral plane motion is controlled by the rudder movement. They have advantages over conventional underwater robots (for example, Autonomous Underwater Vehicle (AUV) and Remotely Operated Vehicle (ROV), for instance, low energy consumption and long-term operational durations. Underwater gliders move with low speed and consequently have low drag. There are widely used in both education and military application in oceanography [2]. The original concept of an underwater glider was proposed by [3]. Various underwater gliders have been extensively developed, for example, Slocum [4], Spray [5] and Seaglider [6]. Figure 1 shows several designs of underwater gliders. Slocum is 3.2 m long and 40 kg displacement. The Slocum glider uses either electric power or thermal powered engine, which was able to operate up to 150 m depth with glide angles from 10° to 40° with longitudinal speed of 0.15 to 0.22 m/s. They are aimed to operate in fleets in a coordinate networks (e.g. monitoring grid, feature tracking, station keeping). Spray has a 2 m long body and weighs 50 kg. Spray glider is a slender ellipsoid shape and uses electrical power. Hull shape is key design for performance. Spray had been successfully tested up to 1500 m depth with operating speed of 0.2 to 0.3 m/s. Seaglider with low drag axisymmetric shape has 1.8 m long body and weighs 52 kg. It uses battery powered is able to operate up to 1500 m depth with travelling speed of 0.25 m/s. Other remarkable glider designs have been also investigated. Those vehicles are ALBAC [7], Rogue [8], SeaExplorer glider [9], USM underwater glider [10] and Sterne sea glider [11].

* Corresponding author: P. Jantapremjit
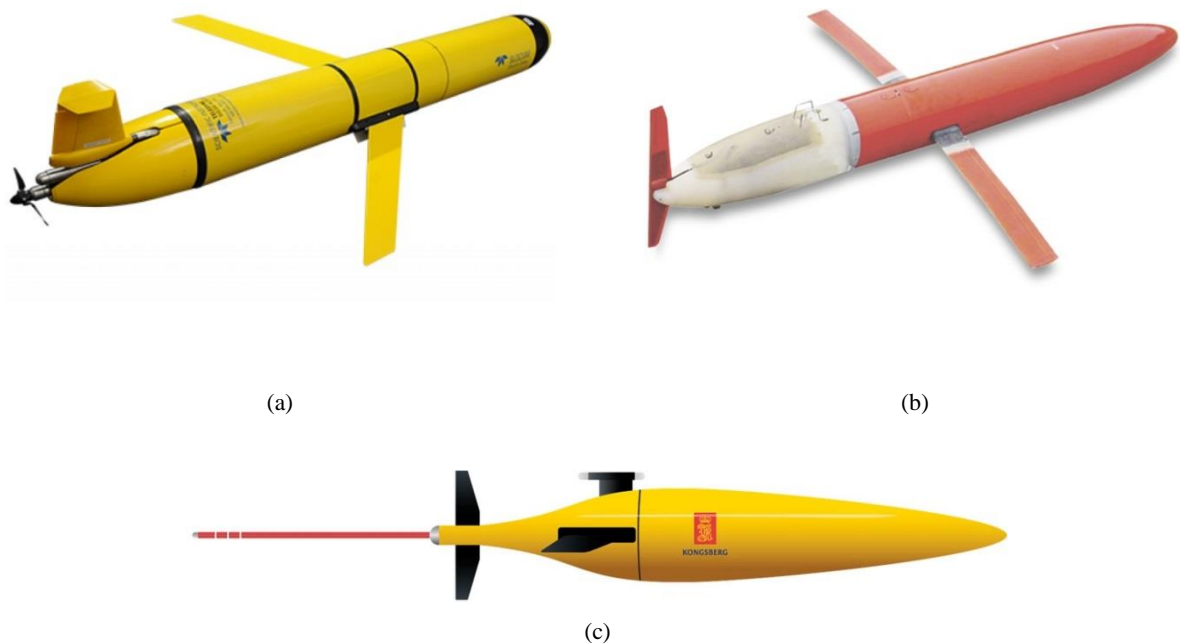E-mail address: pakpong@eng.buu.ac.th

(a)

(b)

(c)

Fig. 1. Underwater gliders: (a) Slocum glider [4] (b) Spray glider [5] (c) Seaglider [6].

Design of a hull shape for an underwater glider is one of the main characteristics in determining the motion behaviour and operational duration. Hull shape design provides hydrodynamics estimation. Currently, various efforts [12-17] are found that investigate hydrodynamic coefficients of underwater vehicles from computational fluid dynamics (CFD) with experimental validation. CFD techniques are used to study the hydrodynamics because of low cost, less time and acceptable result. Most research has been investigated in various issues of hydrodynamics such as grid generation, boundary resolution technique and influence of boundary condition. A multi-objective optimisation design framework [12] integrated with the computer aided design (CAD) and CFD is studied for AUV hydrodynamics in shape geometry variation AUV drag estimation and shape optimization are considered using CFD. An AUV with a ducted propeller [13] was evaluated for estimating hydrodynamic characteristics using CFD. In [14], unstructured mesh and adaptive mesh refinement using commercial CFD software improved efficiency and shown accuracy. Optimisation of hull shape was utitlised with multi-island genetic algorithm. A high lift to drag ratio glider shape, the blended-wing-body [15] was investigate for optimized hydrodynamics parameters using Kriging-base genetic algorithm. Hydrodynamic drag and life parameters were obtained using CFD approach to steady state motion of the torpedo shape underwater glider [16]. Steady state CFD analysis method with automated meshing and parametric hull shape definition of Autosub AUV was investigated [17]. Furthermore, a strip theory and CFD [18] were used for estimating hydrodynamics. Experimental data has been carried out for validating the simulation. Moreover, CFD analysis approach with Hess-Smith's added mass method obtained hydrodynamic coefficients of underwater glider in a saw-tooth path of a vertical motion [19]. Optimal tordepo-like shape AUV moving near free surface was determined using simulated annealing algorithm to reduce the total resistance [20]. Various underwater glider's parameters, for example, drag, power conversion ratio and barycenter offsets were comparing using CFD analysis software [21]. Steady state CFD analysis simulation was used to evaluate the dynamic stability subjected to external disturbances of a low speed underwater glider [22].

In summary, this paper aims to develop hull concept design techniques that are robust and reliable using CFD analysis procedures. Section 2 presents a mathematical model of the underwater glider. Section 3 presents hull shape design and CFD. Section 4 delivers numerical simulation results. Conclusion is given in the last section.

2. MODEL OF AN UNDERWATER GLIDER

2.1 Kinematics and dynamics

In general, kinematics and dynamics model of an underwater glider are similar to the 6-DOFs nonlinear equation of an underwater vehicle. The notation used in this work defined by SNAME [23]. They are obtained by using a global reference of the NED-frame and the body-fixed frame (see Fig. 2).

The kinematic model of an underwater glider is defined as,

$$\dot{\eta} = J(\eta)v \tag{1}$$

The rotation and transformation matrix of the Euler angle is obtained by,

$$J(\eta) = \begin{bmatrix} R_b^n(\eta) & 0_{3\times3} \\ 0_{3\times3} & T_b^n(\eta) \end{bmatrix} \tag{2}$$

The dynamics model derived from the Newton-Euler equation is,

$$M\dot{v} + C(v)v + D(v)v + g(\eta) = \tau \tag{3}$$

2.2 Equation of motion

Equation of motion of an underwater vehicle is 6-DOFs nonlinear equation of motion [23, 24]. The mode of an underwater glider is similarly suggested in [25]. From Fig. 2, the vertical motion equation is simplified by neglecting the diagonal and coupling terms and tether dynamics. It is assumed that added masses are constant. The contribution of wings is dominated by the lift and drag forces during a low angle of attack because the glider body is symmetry.
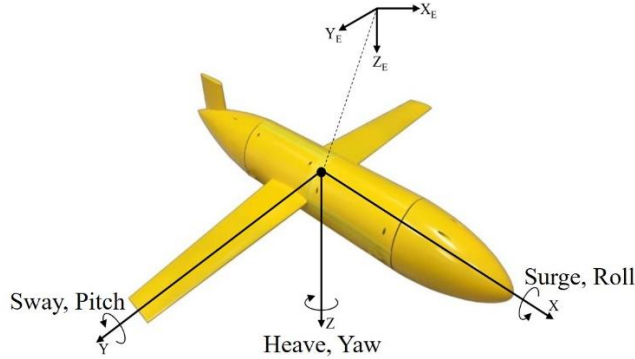

Fig. 2. Frame coordinates of an underwater glider

The equation of motion of an underwater glider is given as follows,

$$
\begin{aligned}
m\left(\dot{u} - vr + wq - x_g(q^2 + r^2) + y_g(pq - \dot{r}) + z_g(pr + \dot{q})\right) &= X \\
m\left(\dot{v} - wp + ur - y_g(r^2 + p^2) + z_g(qr - \dot{p}) + x_g(qp + \dot{r})\right) &= Y \\
m\left(\dot{w} - uq + vp - z_g(p^2 + q^2) + x_g(rp - \dot{q}) + y_g(rq + \dot{p})\right) &= Z
\end{aligned}
\tag{4}
$$

$$
\begin{aligned}
I_x\dot{p} + (I_z - I_y)qr - (\dot{r} + pq)I_{xz} + (r^2 - q^2)I_{yz} + (pr - \dot{q})I_{xy} + m(y_g(\dot{w} - uq + vp) - z_g(\dot{v} - wp + ur)) &= K \\
I_y\dot{q} + (I_x - I_z)rp - (\dot{p} + qr)I_{xy} + (p^2 - r^2)I_{zx} + (qp - \dot{r})I_{yz} + m(z_g(\dot{u} - vr + wq) - x_g(\dot{w} - uq + vp)) &= M \\
I_z\dot{r} + (I_y - I_x)pq - (\dot{q} + rp)I_{yz} + (q^2 - p^2)I_{xy} + (rq - \dot{p})I_{zx} + m(x_g(\dot{v} - wp + ur) - y_g(\dot{u} - vr + wq)) &= N
\end{aligned}
\tag{5}
$$

2.3 Vectorial representaion

A) Inertial matrix

According to [24], inertial matrix is composed of the rigid body inertial matrix and rigid body-like hydrodynamic added mass. It can be written as,

$$
M = \begin{bmatrix}
m & 0 & 0 & 0 & mz_g & -my_g \\
0 & m & 0 & -mz_g & 0 & mx_g \\
0 & 0 & m & my_g & -mx_g & 0 \\
0 & -mz_g & my_g & I_x & -I_{xy} & -I_{xz} \\
mz_g & 0 & -mx_g & -I_{yx} & I_y & -I_{yz} \\
-my_g & mx_g & 0 & -I_{zx} & -I_{zy} & I_z
\end{bmatrix}
-
\begin{bmatrix}
X_{\dot u} & X_{\dot v} & X_{\dot w} & X_{\dot p} & X_{\dot q} & X_{\dot r} \\
Y_{\dot u} & Y_{\dot v} & Y_{\dot w} & Y_{\dot p} & Y_{\dot q} & Y_{\dot r} \\
Z_{\dot u} & Z_{\dot v} & Z_{\dot w} & Z_{\dot p} & Z_{\dot q} & Z_{\dot r} \\
K_{\dot u} & K_{\dot v} & K_{\dot w} & K_{\dot p} & K_{\dot q} & K_{\dot r} \\
M_{\dot u} & M_{\dot v} & M_{\dot w} & M_{\dot p} & M_{\dot q} & M_{\dot r} \\
N_{\dot u} & N_{\dot v} & N_{\dot w} & M_{\dot p} & M_{\dot q} & M_{\dot r}
\end{bmatrix}
\tag{6}
$$

B) Coriolis and centripetal matrix

Coriolis and centripetal matrix are derived from system inertial matrix. They combine rigid body Coriolis-Centripetal matrix and hydrodynamic Coriolis-Centripetal matrix. They can be expressed as,

$$
C(v) = \begin{bmatrix}
0_{3\times3} & -S(M_{11}v_1 + M_{12}v_2) \\
-S(M_{11}v_1 + M_{12}v_2) & -S(M_{21}v_1 + M_{22}v_2)
\end{bmatrix}
+
\begin{bmatrix}
0_{3\times3} & -S(A_{11}v_1 + A_{12}v_2) \\
-S(A_{11}v_1 + A_{12}v_2) & -S(A_{21}v_1 + A_{22}v_2)
\end{bmatrix}
\tag{7.1}
$$

where the hydrodynamic Coriolis-Centripetal matrix is defined as,

$$
C_A(v) = \begin{bmatrix}
0 & 0 & 0 & 0 & -a_3 & a_2 \\
0 & 0 & 0 & a_3 & 0 & -a_1 \\
0 & 0 & 0 & -a_2 & a_1 & 0 \\
0 & -a_3 & a_2 & 0 & -b_3 & b_2 \\
a_3 & 0 & -a_1 & b_3 & 0 & -b_1 \\
-a_2 & a_1 & 0 & -b_2 & b_1 & 0
\end{bmatrix}
\tag{7.2}
$$

and

$$
\begin{aligned}
a_1 &= X_{\dot u}\,u + X_{\dot v}\,v + X_{\dot w}\,w + X_{\dot p}p + X_{\dot q}q + X_{\dot r}\,r & b_1 &= K_{\dot u}\,u + K_{\dot v}\,v + K_{\dot w}\,w + K_{\dot p}p + K_{\dot q}q + K_{\dot r}\,r \\
a_2 &= Y_{\dot u}\,u + Y_{\dot v}\,v + Y_{\dot w}\,w + Y_{\dot p}p + Y_{\dot q}q + Y_{\dot r}\,r & b_2 &= M_{\dot u}\,u + M_{\dot v}\,v + M_{\dot w}\,w + M_{\dot p}p + M_{\dot q}q + M_{\dot r}\,r \\
a_3 &= Z_{\dot u}\,u + Z_{\dot v}\,v + Z_{\dot w}\,w + Z_{\dot p}p + Z_{\dot q}q + Z_{\dot r}\,r & b_3 &= N_{\dot u}\,u + N_{\dot v}\,v + N_{\dot w}\,w + N_{\dot p}p + N_{\dot q}q + N_{\dot r}\,r
\end{aligned}
\tag{7.3}
$$

C) Damping matrix

Damping matrix is a collection of other hydrodynamic forces and moment which is the quadratic lift and drag,

$$
D(v) = -\mathrm{diag}\{X_u, Y_v, Z_w, K_p, M_q, N_r\} - \mathrm{diag}\{X_{u|u|}|u|, Y_{v|v|}|v|, Z_{w|w|}|w|, K_{p|p|}|p|, M_{p|p|}|p|, N_{r|r|}|r|, \}
\tag{8}
$$

D) Restoring force matrix

A vehicle is affected by the gravity and buoyancy forces. It is expressed as,

$$
g(\eta) = [f_b + f_g \quad r_b \times f_b + r_g \times f_g]^T
\tag{9}
$$

where f_b, f_g are buoyancy force and gravitational force and r_b, r_g are position vectors of the centre of buoyancy/gravity with respect to the centre of origin.

3. HULL DESIGN

3.1 Hull geometry

Hull shape parameters of the glider are defined by [20]. The body comprises of a nose and a tail section that are connected with a middle hull section (see Fig. 3). Nose and tail radii are given by,

$$r_n = \frac{d}{2}\left(1 - \left(\frac{x - l_t - l_m}{l_n}\right)^{n_n}\right)^{\frac{1}{n_n}}, \qquad r_t = \frac{d}{2}\left(1 - \left(\frac{l_t - x}{l_t}\right)^{n_t}\right) \tag{10}$$

where n_n, n_t are two exponents and r_n, r_t are the radius at the nose and tail section at position x and d is the diameter of the middle hull section. The length of the middle hull section l_m is obtained with a volume constraint.
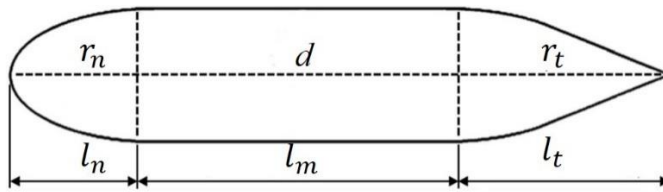

Fig. 3. Parameters of the hull geometry

For a particular example, the hull shape of the Slocum glider is now considered. Two designs of glider's hull are investigated for the minimum total resistance. Figure 4 exhibits the comparison geometry of the hull shape. Table 1 shows hull parameters in this study.
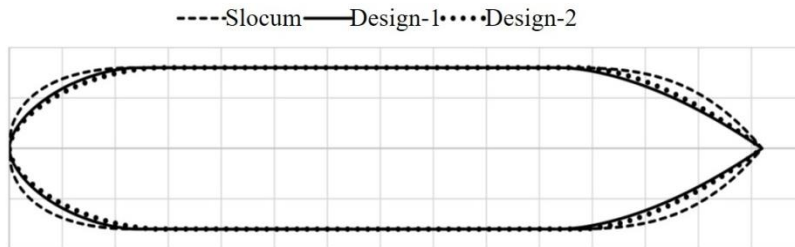

Fig. 4. Hull shape of the Slocum glider and two designs

Table 1: Hull design parameters

Parameters	Slocum [4]	Design-1	Design-2
l_n	240 mm	240 mm	240 mm
l_m	800 mm	800 mm	800 mm
l_t	380 mm	380 mm	380 mm
l	1,420 mm	1,420 mm	1,420 mm
d	160 mm	160 mm	160 mm
n_n	2.3	1.7	1.5
n_t	3	1.7	1.5
V	0.0245 m^3	0.0227 m^3	0.0224 m^3

3.2 Flow analysis

In this study, the fluid created around a glider's hull is incompressible water [26]. The Reynold Average Navier Stokes (RANS) equation is used to define the flow field ($U_i = u, v, w$) and the pressure (P) around a vehicle's hull [22],

$$\frac{\partial \bar{U}_i}{\partial x_i} = 0$$

$$\frac{\partial \bar{U}_i}{\partial t} + u_i \frac{\partial \overline{U_i U_j}}{\partial x_i} = \frac{1}{\rho} \frac{\partial P}{\partial x_i} + \frac{\partial}{\partial x_j}\left(v\left(\frac{\partial \bar{U}_i}{\partial x_j} + \frac{\partial \bar{U}_j}{\partial x_i}\right)\right) - \frac{\partial \overline{u_i u_j}}{\partial x_j} + f_i$$

(11)

Various turbulence models are used to provide solution to the Reynolds stresses. The $k - \omega$ sheer stress transport (SST) is commonly used for turbulence model due to its robustness and cost effectiveness. For the steady state drift tests, the fluid domain consists of the glider model, flow velocity inlet, zero relative pressure outlet, ceiling, bottom wall and two free slip walls. Figure 5 shows the entire computational domain. The location of the glider model is defined 1.0 time body length from the flow inlet and 4.0 times body length from the outlet. The ceiling, bottom and side walls are 0.5 time body length from the wall.
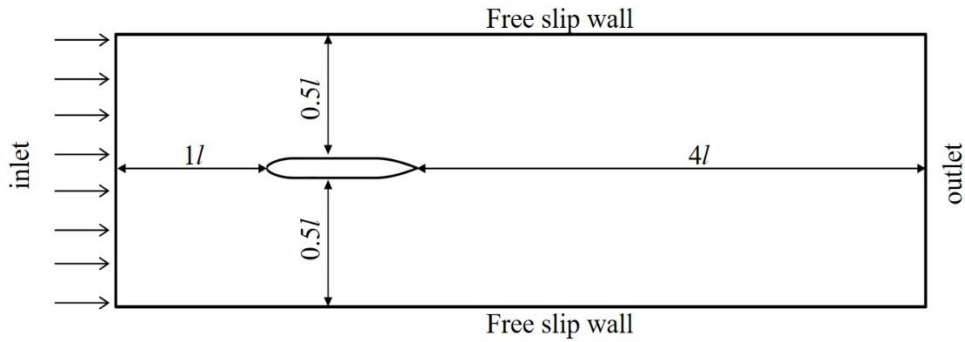

Fig. 5. Boundary condition for the numerical drift test

The mesh parameter is very important. The boundary layer was estimated using the following equation,

$$\delta = 0.035 L R e^{-1/7}$$

(12)

and the first layer thickness Δy^+ can be estimated from [22],

$$\Delta y = L \Delta y^+ \sqrt{80}\, Re^{-13/14}$$

(13)

The coefficients are used to described the hydrodynamic forces of the glider,

$$C_d = \frac{F_x}{0.5\rho S_a U^2}$$

(14.1)

$$C_l = \frac{F_y}{0.5\rho S_a U^2}$$

(14.2)

$$C_m = \frac{F_z}{0.5\rho S_a L_a U^2}$$

(14.3)

where C_d, C_l and C_m are the coefficients of drag, lift and pitch moment of the glider, respectively. S_a is the maximum cross-section area of the glider shape. Furthermore, mesh quality is vital. This is essential for archiving the accuracy and stable requirements of the numerical simulation. Optimal number of elements can be used from a grid dependence test. Table 2 shows the numerical calculation of the grid dependence test using CFD software. Obviously, Grid #3 and Grid #4 are satisfactory for using in the numerical simulation. The entire layer mesh of Slocum was shown in Fig. 6(a). A refine mesh at nose and tail sections is used in this study is shown in Fig. 6(b).
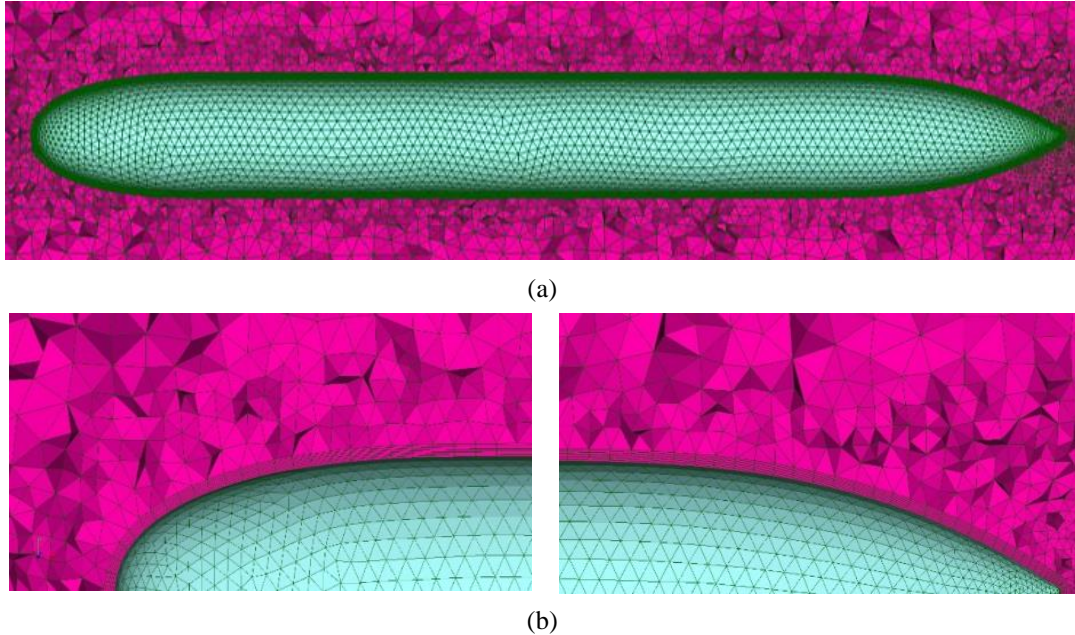

(a)

(b)

Fig. 6. Boundary layer refined mesh of Slocum glider (a) whole body
(b) trimmer at nose (left) and tail (right) sections

Figure 7 selectively shows a comparison of the longitudinal section view of computational mesh around the design-1 and design-2 gliders. The CFD model is validated with the experimental measured drag of the glider with no-wave condition. Figure 8 shows the Slocum's drag coefficient of the CFD study which is in good agreement with the experimental study [12] with a maximum relative error of 1.5% at $Re = 1.79 \times 10^6$ and a minimum relative error of 0.1% at $Re = 0.59 \times 10^6$.

Table 2: Grid dependence test of the Slocum glider at speed of 1 m/s

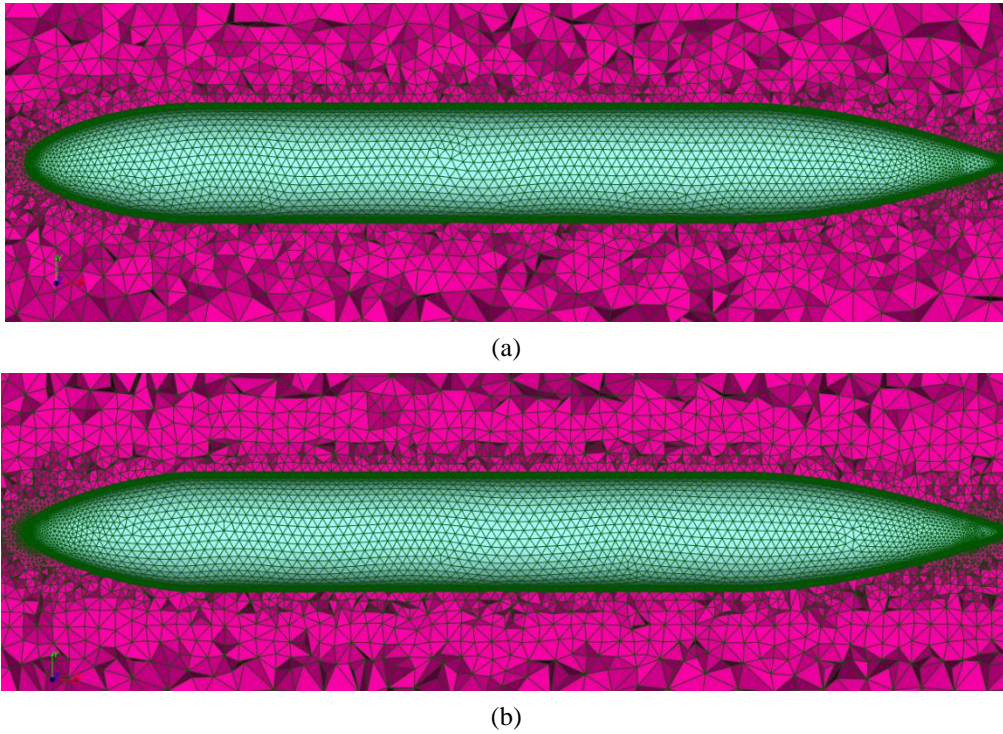| Grid	Number of elements	C_d
Grid #1	214,512	0.00537
Grid #2	228,483	0.00514
Grid #3	242,381	0.00510
Grid #4	256,279	0.00510
Grid #5	270,104	0.00509
Grid #6	284,002	0.00507
Grid #7	297,973	0.00508

(a)

(b)

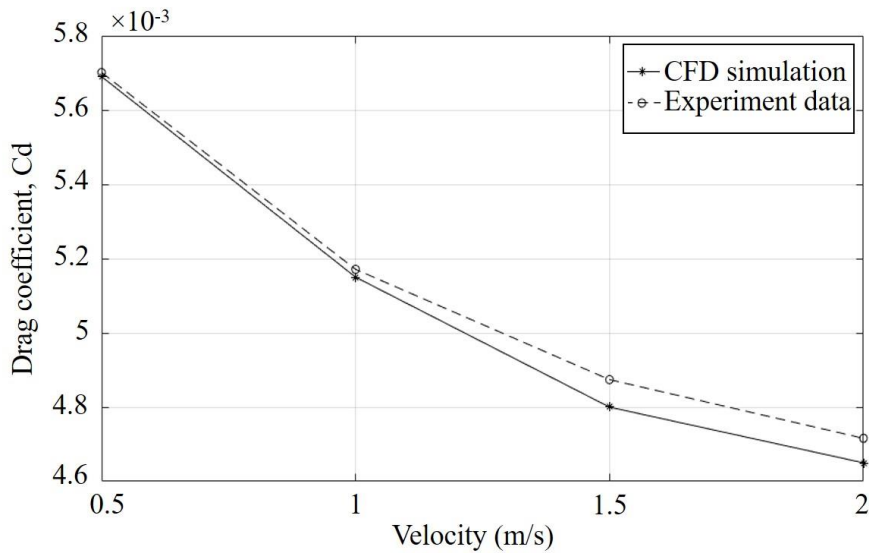**Fig. 7**. Boundary layer refined mesh of (a) design-1 (b) design-2

Fig. 8. Comparison of drag coefficient using CFD and from experiment [20]

The velocities (0.5, 1.0, 1.5 and 2 m/s) were used in experiment [20], the drag and drag coefficients of three designs are then compared with the CFD software. These results (see Fig. 9) show that drag coefficients of the design-1 and design-2 are lower than that of the Slocum glider. At speed of 1 m/s the drag coefficients of design-1 and design-2 is about 6.8% and 7.2% smaller than that of the Slocum. The volume of the design-1 is a little bit larger than that of the design-2. Furthermore, the velocity profile shows the wake occurred in design-2.
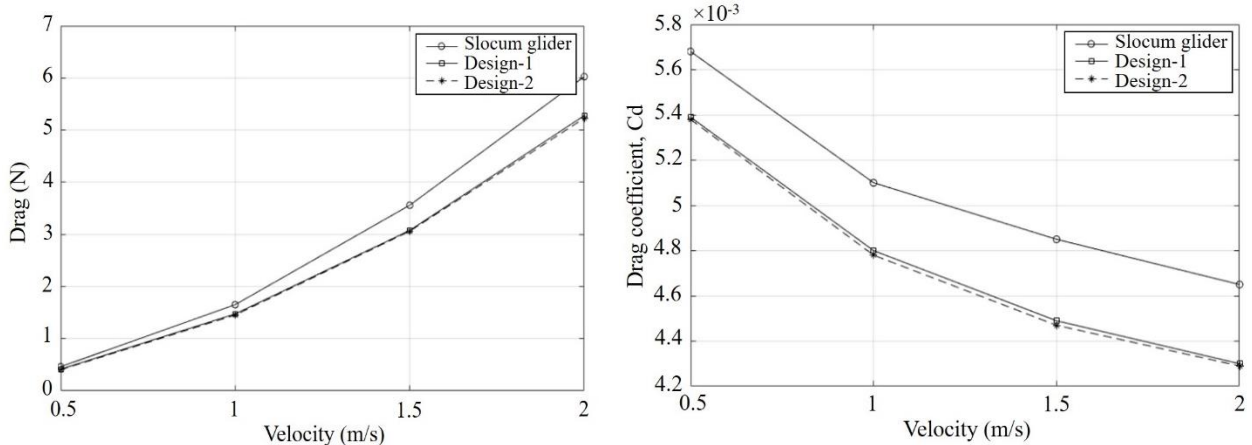
Fig. 9. Comparison of drag calculation using CFD for various designs

3.3 Performance

Energy consumption is another criterion to be considered for evaluating the performance of the glider. The power usage proposed by [21] is then simplified as,

$$e = F_d v \qquad (15)$$

where F_d is the drag force and v is the velocity of the glider.

4. SIMULATION RESULTS

4.1 CFD analysis

Using CFD simulation for the design-1 glider in the steady state and incompressible flow, the hydrodynamic coefficients, flow behavior, force distribution and pressure distribution on the glider for velocities (0.05, 0.10, 0.15, 0.20, 0.25, 0.30 m/s) and angle of attack (α = -10 to 10 in the step of 2 degrees) are obtained. The design-1 hull shape is used for the study.

4.2 Drift tests

The fluid domain is defined as a cuboid fixed in space as previously shown in Fig. 5. The results in Fig. 10-11 show the effect of attack angle on the life and drag coefficient in various velocities. High lift to drag is desirable for a glider which the result is shown in Fig. 12. It shows the maximum L/D ratio is about 2 at $\alpha = 16°$ at the velocity of 0.25-0.3 m/s. Figure 13 shows the effect of attack angle and velocity on pitching moment coefficients.
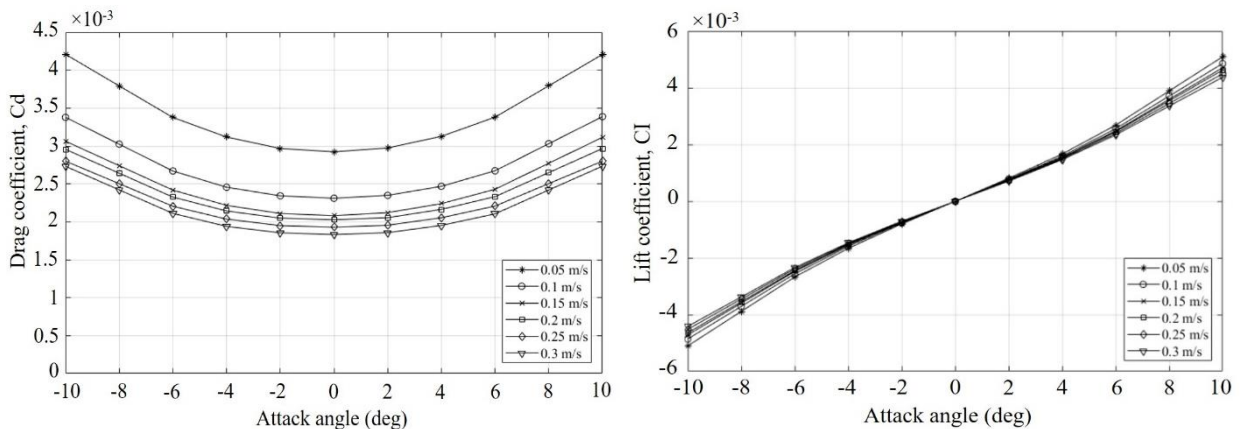

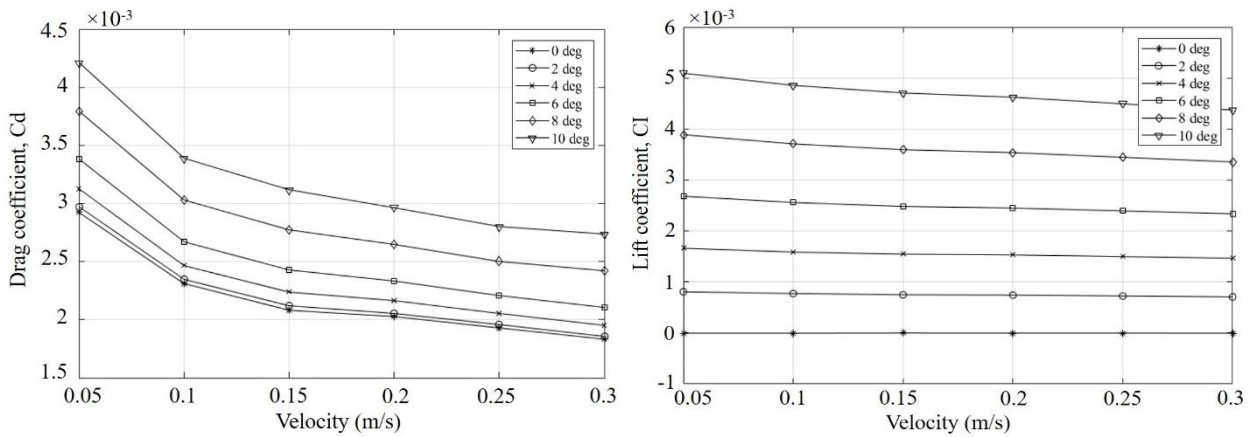Fig. 10. Comparison of drag and lift coefficients as function of attack angle for design-1

Fig. 11. Comparison of drag and lift coefficients as function of velocity for design-1
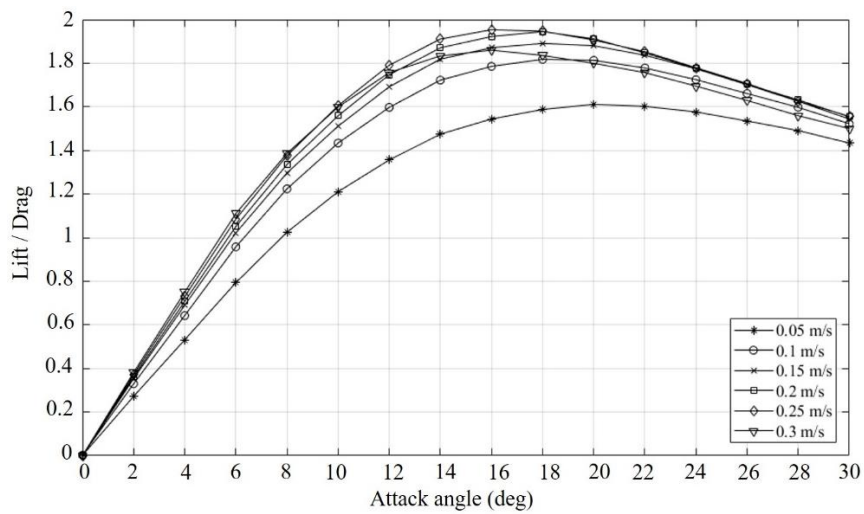

Fig. 12. Lift to drag ratio as function of attack angle for design-1
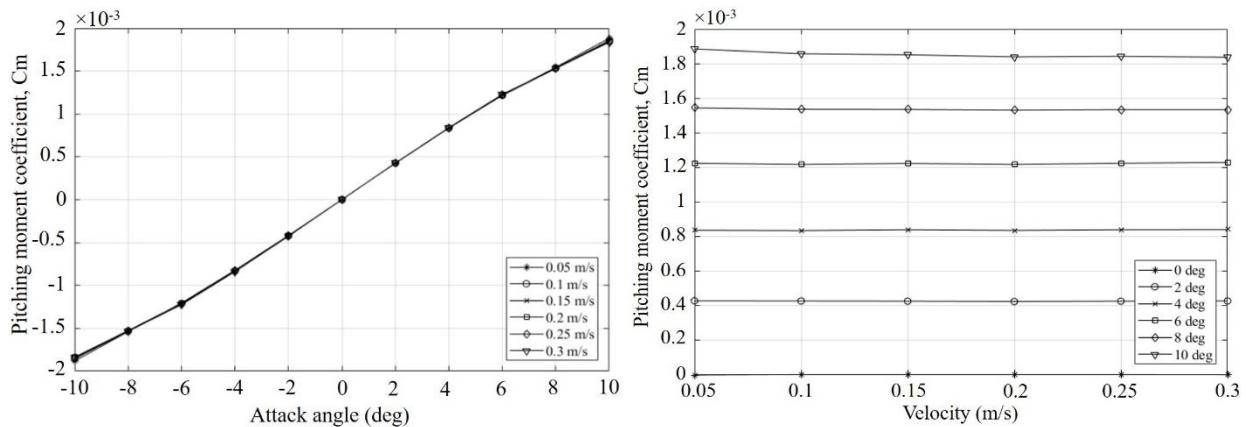

Fig. 13. Comparison of pitching moment coefficient as function of attach angle and velocity for design-1

4.3 Hydrodynamics coefficients

The results compare the variation in fluid velocity around the hull at the attack angle of 0° of the heave force with pitch and velocity (see Fig. 14) and the heave moment with pitch and heave velocity (see Fig. 15).
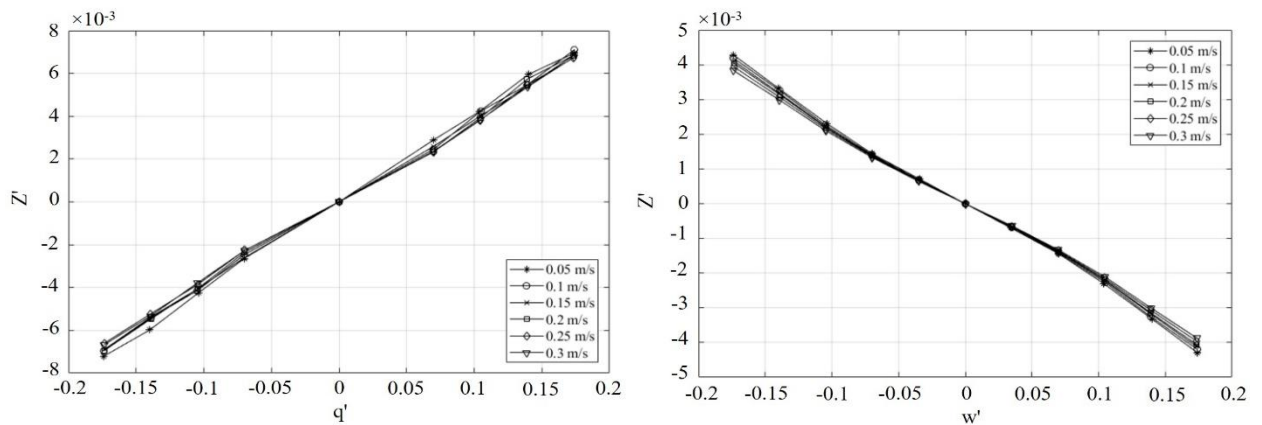
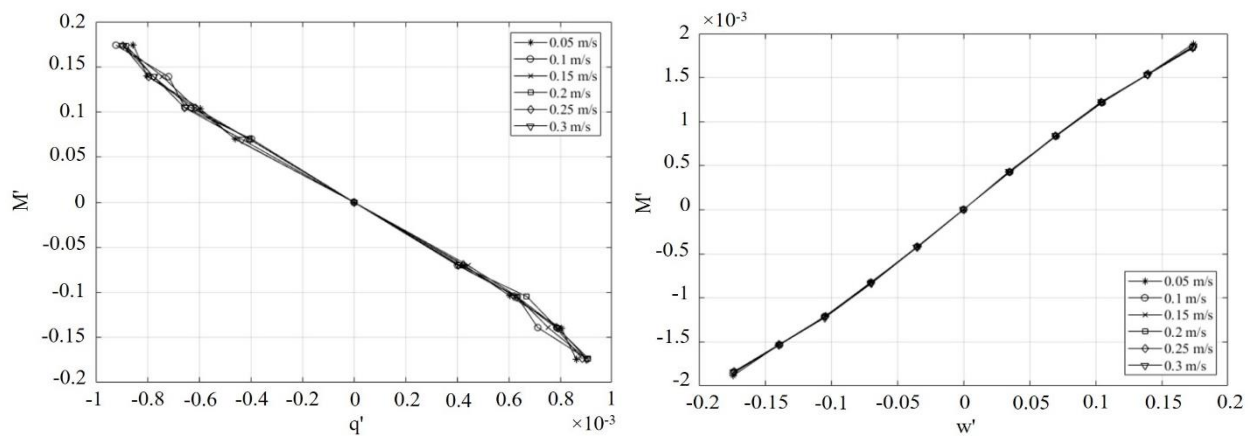**Fig. 14**. Variation of heave force with pitch and heave velocity

Fig. 15. Variation heave moment with pitch and heave velocity

4.4 Power usage

The total power usage of the Slocum and design-1 glider is computed and shown in Fig. 16. Power usage of the design-1 is about 5.76% and 11.12% smaller than that of the Slocum at the velocity of 1 m/s and 2 m/s, respectively.
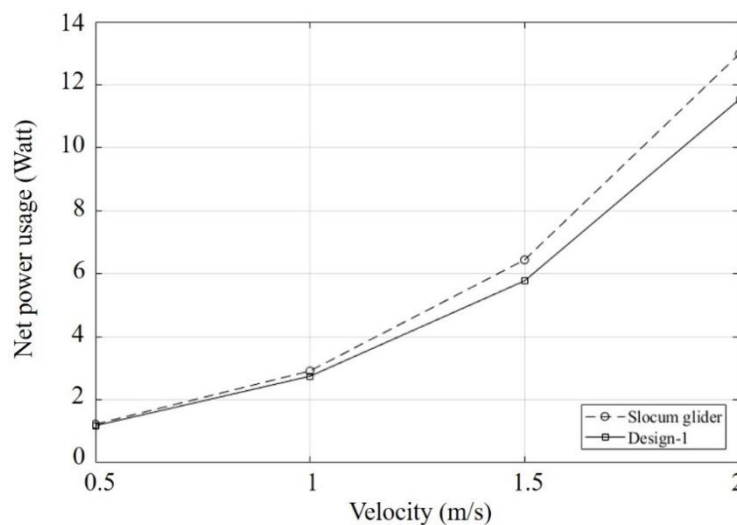

Fig. 16. Comparison of net power usage

5. Conclusion

In conclusion, this work investigates the numerical calculation of hydrodynamic coefficient of the underwater gliders' hull shape using CFD with RANS with SST turbulence model. The total resistance of the designed hull geometry reduces by 7% whereas the design's volume is similar to the Slocum glider. The results show that the drag coefficients calculating from CFD reasonably agree with the experimental work. Both lift and drag coefficient are increased when the attack angle is increased and the highest lift/drag ratio occurred when the attack angle is $\alpha = 16°$ at a velocity of 3.0 m/s. Numerical prediction of the hydrodynamics show how the heave force-pitch velocity, heave force-heave velocity, heave moment-pitch velocity and heave moment-heave velocity are related. These hydrodynamic derivatives are also in accordance with physical behaviour of the undersea glider. The variation of hydrodynamics trends is not much different for the studied velocity. It is obvious that the energy consumption for the proposed design is marginally lower than that of the Slocum. The performance is quite well. Therefore, future work needs to study the performance of the underwater glider with wings under the waves.

Nomenclature

$C(v)$	Coriolis and centripetal matrix
C_d	Drag coefficient
C_l	Lift coefficient
C_m	Pitch moment coefficient
$D(v)$	Hydrodynamic damping and lift matrix
$g(\eta)$	Gravity and buoyancy forces and moment matrix
I_x, I_y, I_z	Inertia matrix with respect to the x, y, z -axis
$[K, M, N]$	Moment of external force vectors about origin in the body-fixed frame
M	Inertia and added inertia matrix
$[p, q, r]$	Angular velocity vectors about origin in the body-fixed frame
$R_b^n(\eta)$	Linear velocity transformation
$S(\cdot)$	Skew-symmetric matrix
$T_b^n(\eta)$	Angular velocity transformation
$[u, v, w]$	Translational motion vectors along the x, y, z -axes
$[X, Y, Z]$	External force vectors about origin in the body-fixed frame
X_u	Hydrodynamic added mass coefficient, the force X along the x-axis due to a velocity u
$X_{\dot{u}}$	Hydrodynamic added mass coefficient, the force X along the x-axis due to an acceleration $\dot{u}$
$X_{u\|u\|}$	Hydrodynamic damping coefficient defined using SNAME notation
Re	Reynolds number
δ	Boundary layer
η	Position and attitude vector
τ	External force and moment input vector
v	Linear and angular velocity vector

References

[1] Wood, S. Autonomous underwater gliders, Underwater Vehicles, 2009, IntechOpen.

[2] Wynn, R.B., Huvenne, V.A.I., Bas, T.P.L., Murton, B.J., Connelly, D.P., Bett, B.J., Ruhl, H.A., Morris, K.J., Peakall, J., Parsons, D.R., Sumner, E.J., Darby, S.E., Dorrell, R.M. and Hunt, J.E. Autonomous Underwater Vehicles (AUVs): Their past, present and future contributions to the advancement of marine geoscience, Marine Geology, Vol. 352, 2014, pp. 451-468.

[3] Stommel, H. The Slocom mission, Oceanograph, Vol. 2(1), 1989, pp. 22-25.

[4] Webb, D.C., Simonetti, P.J. and Jones, C.P. SLOCUM: an underwater glider propelled by environmental energy, IEEE Journal of Oceanic Engineering, Vol. 26(4), 2001, pp. 447-452.

[5] Sherman, J., Davis, R.E., Owens, W.B. and Valdes, J. The autonomous underwater glider "Spray", IEEE Journal of Oceanic Engineering, Vol. 26(4), 2001, pp. 437-446.

[6] Eriksen, C.C., Osse, T.J., Light, R.D., Wen, T., Lehman, T.W., Sabin, P.L., Ballard, J.W. and Chiodi, A.M. Seaglider: a long-range autonomous underwater vehicle for oceanographic research, IEEE Journal of Oceanic Engineering, Vol. 26(4), 2001, pp. 424-436.

[7] Kawaguchi, K., Ura, T., Tomoda, Y. and Kobayashi, H. Development and sea trials of a shuttle type AUV "ALBAC", International Symposium on Unmanned Untethered Submersible Technology, 1993, pp. 7-13.

[8] Leonard, N.E. and Graver, J.G. Model-based feedback control of autonomous underwater gliders, IEEE Journal of Oceanic Engineering, Vol. 26(4), 2001, pp. 633-645.

[9] Claustre, H., Beguery, L. and Patrice, P. SeaExplorer glider breaks two world records : multisensor UUV achieves blobal milestones for endurance, distance, Sea Technology, Vol. 55, 2014, pp. 19-22.

[10] Hussain, N.A.A., Chung, T.M., Arshad, M.R., Mohd-Mokhtar, R. and Abdullah, M.Z. Design of an underwater glider platform for shallow-water applications, International Journal of Intelligent Defence Support Systems, Vol. 3, 2010, pp. 186-206.

[11] Sliwka, J., Clement, B. and Probst, I. Sea glider guidance around a circle using distance measurements to a drifting acoustic source, IEEE/RSJ International Conference on Intelligent Robots and Systems, 2012, pp. 94-99.

[12] Vasudev, K.L., Sharma, R. and Bhattacharyya, S.K. A multi-objective optimization design framework integrated with CFD for the design of AUVs, Methods in Oceanography, Vol. 10, 2014, pp. 138-165.

[13] Joung, T.-H., Sammut, K., He, F. and Lee, S.-K. Shape optimization of an autonomous underwater vehicle with a ducted propeller using computational fluid dynamics analysis, International Journal of Naval Architecture and Ocean Engineering, Vol. 4(1), 2012, pp. 44-56.

[14] Gao, T., Wang, Y., Pang, Y. and Cao, J. Hull shape optimization for autonomous underwater vehicles using CFD, Engineering Applications of Computational Fluid Mechanics, Vol. 10(1), 2015, pp. 599-607.

[15] Sun, C., Song, B. and Wang, P. Parametric geometric model and shape optimization of an underwater glider with blended-wing-body, International Journal of Naval Architecture and Ocean Engineering, Vol. 7(6), 2015, pp. 995-1006.

[16] Singh, Y., Bhattacharyya, S.K. and Idichandy, V.G. CFD approach to modelling, hydrodynamic analysis and motion characteristics of a laboratory underwater glider with experimental result, Journal of Ocean Engineering and Science, Vol. 2(2), 2017, pp. 90-119.

[17] Phillips, A., Furlong, M. and Turnock, S.R. The use of computational fluid dynamics to determine the dynamic stability of an autonomous underwater vehicle, Oceans 2007, Aberdeen, 2007, pp. 1-6.

[18] Isa, K., Arshad, M.R. and Ishak, S. A hybrid-driven underwater glider model, hydrodynamics estimation, and an analysis of the motion control, Ocean Engineering, Vol. 81, 2014, pp. 111-129.

[19] Yang, L., Cao, J., Cao, J., Yao, B., Zeng, Z. and Lian, L. Hydrodynamic and vertical motion analysis of an underwater glider, Oceans 2016, Shanghai, 2016, pp. 1-6.

[20] Alvarez, A., Bertram, V. and Gualdesi, L. Hull hydrodynamic optimization of autonomous underwater vehicles operating at snorkeling depth, Ocean Engineering, Vol. 36(1), 2009, pp. 105-112.

[21] Chen, Y.-j., Chen, H.-x. and Ma, Z. Hydrodynamic analyses of typical underwater gliders, Journal of Hydrodynamics, Vol. 27(4), 2015, pp. 556-561.

[22] Javaid, M.Y., Ovinis, M., Hashim, F.B.M., Maimun, A., Ali, S.S.A. and Ahmed, S.A. Investigation on the dynamic stability of an underwater glider using CFD simulation, IEEE 6th International Conference on Underwater System Technology: Theory & Applications, Penang, 2016, pp. 230-235.

[23] SNAME. Nomenclature for treating the motion of a submerged body through a fluid, Technical and research bulletin. 1952, New York: The Society of Naval Architects and Marine Engineers.

[24] Fossen, T.I. Handbook of Marine Craft Hydrodynamics and Motion Control, 2011: John Wiley & Sons, Ltd.

[25] Graver, J.G. Underwater Gliders: Dynamics, Control and Design, Ph.D. Thesis. 2005, Princeton University.

[26] Du, X.-x., Wang, H., Hao, C.-z. and Li, X.-l. Analysis of hydrodynamic characteristics of unmanned underwater vehicle moving close to the sea bottom, Defence Technology, Vol. 10, 2014, pp. 76-81.